Number 5 Volume 19 may 2013 Journal of Engineering

Experimental Study of Power Increase Transient in Heat Generation Systems Simulated By Immersed Heat Source

Dr. Akram W. Ahmed Ezzat
Asst. prof. Dept. of Mech. Eng.
Baghdad University
Email: akram whabi@yahoo.com

Sarmad A. Abdul Hussain
Dept. of Mech. Eng.
Baghdad University
Email: akram whabi@yahoo.com

ABSTRACT

Theoretical and experimental investigations of the transient heat transfer parameters of constant heat flux source subjected to water flowing in the downward direction in closed channel are conducted. The power increase transient is ensured by step change increase in the heat source power. The theoretical investigation involved a mathematical modeling for axially symmetric, simultaneously developing laminar water flow in a vertical annulus. The mathematical model is based on one dimensional downward flow. The boundary conditions of the studied case are based on adiabatic outer wall, while the inner wall is subjected to a constant heat flux. The heat & mass balance equation derived for specified element of bulk water within the annulus and solved by using Laplace method to determine the variation of bulk water temperature. The experimental investigation included a set of experiments carried out to investigate the temperature variation along the heat source for power increase transient of (5%, 10%, 15% and 20%) of its nominal value during and after reaching the steady state condition. Estimation of the boiling safety factor is predicted and compared with the theoretical values. Reliable agreement between experimental and theoretical approaches is reached. The later showed that the elapsed time required for the clad surface temperature to reach its steady state values after each transient is less than that related to bulk water temperature. New correlation for prediction of critical heat flux, CHF based on inlet water temperature and water mass flux are investigated and compared with CHF correlations obtained from previous researches. Specific recommendations concerned with preventive measured required to eliminate the effect of boiling crisis are concluded based on theoretical and experimental results related to transients setting times obtained from each case study.

KEYWORDS: CHFprediction, Sub-cooled flow boiling, Heat transfer parameters, Nucleate boiling, Concentric annular channel.

.

دراسة تجريبية للحالة العابرة لزيادة الطاقة في انظمة التوليد الحرارية من خلال تمثيله بمصدر حراري مغمور

سرمد عزيز عبد الحسين
قسم الهندسة الميكانيكية
جامعة بغداد

أ.م.د. أكرم وهبي احمد عزت
قسم الهندسة الميكانيكية
جامعة بغداد

تم أجراء بحث نظري وتجريبي للعناصر الاستدلالية على أنتقال الحراره العابرة لمصدر حراري ثابت الفيض خاضع لجريان الماء نحو الاسفل في قناة مغلقة. تم زيادة الطاقة العابرة من خلال زيادة درجية في الفيض الحراري للمصدر. البحث النظري تضمن نموذج رياضي لتجويف حلقي عمودي متناظر محوريا يكون فيه جريان الماء فيه طباقي متطور. الشروط الحديه لهذه الدراسه كانت تعتمد على أساس جدار خارجي معزول حراريا في حين يتعرض الجدار الداخلي لتدفق حراري ثابت. تم اشتقاق معادلة التوازن الحراري والكتلي لعنصر محدد داخل مجرى الجريان وذلك بأستخدام طريقة لابلاس لتحديد التباين في درجة حرارة الماء. شمل البحث العملي مجموعة من التجارب التي اجريت للبحث في قيم درجة حرارة السطح على طول المصدر الحراري لزيادة طاقة عابرة بنسبة مئوية (5٪، 10٪، 15٪ و 20٪) من القيمة الفعلية خلال وبعد الوصول الى حالة الأستقرار. كذلك

تضمن البحث العملي حساب عامل الأمان للغليان من خلال التنبأ بقيمته ومقارنته مع القيم التي تم الحصول عليها من الجانب النظري. المقارنة جيدة بين النتائج العملية والنظرية فقد تبين أن الزمن اللازم درجة حرارة سطح المصدر الحراري لوصول الى الحالة المستقرة هي أقل من تلك اللازمة

لوصول درجة حرارة الماء الى حالة الأستقرار، وتم وضع معادلات مناسبة لكل منهما. تم التنبأ بقيمة التدفق الحراري الحرج ووضع معادلات خاصة بذلك ومقارنته مع العلاقات الرياضية الخاصة بالابحاث السابقه ضد الفرق في درجة حرارة الدخول والخروج وكذلك التدفق الكتلي للماء. أظهرت نتائج المقارنة مطابقة مقبولة تم وضع أستنتاجات ذات علاقة بالخطوات اللازمة للتقليل من أثار أزمة الغليان أستنادا الى النتائج النظرية والعملية المتعلقة بتحديد الأوقات اللازمة للوصول الى الحالات المستقرة بعد كل حالة عابرة

الكلمات الرئيسية: تنبأ معدل التدفق الحراري، ظاهرة الغليان لجريان مائع، خواص انتقال الحرارة، غليان النوى، قناة حلقية متماثلة

INTRODUCTION

During safety analysis of any heat generation system it is necessary to demonstrate how far are the limits and conditions established to prevent anticipated transients and ensure plant integrity. The effect of heat power increase transients (HPIT) in power generated system is studied thoroughly to explain its practical significance in flow boiling systems**.** The study becomes very important because it represents an engineering foundation to ensure the safety of the heat generation systems from the initialing events that may take place and lead to rapid temperature build up during the transient course. One of these main consequences that possibly take place is the critical heat flux phenomenon **(CHF**) or also called the "boiling crisis". **CHF** is a phenomenon that denotes the sudden drop of the boiling heat transfer coefficient which results from the replacement of liquid by vapor near the boiling surface. The transient boiling heat transfer is of great importance in analyzing thermo hydrodynamic characteristics of many thermal engineering systems such as petrochemical and nuclear power plants. The transient boiling phenomenon sometimes occurs in the steps of started-up and shut-down of the boiling systems. Power transient occurs when the heat generation rate or heat input varies with time. Generally, an increasing power transient is potentially disastrous and chaotic and is thus more important than a decreasing power transient. Figure (1) shows the heat transfer characteristics during sub-cooled flow boiling of a pure liquid. The onset nucleate boiling (**ONB)** location was identified by visual observations as well as temperature and heat flux data. For the given set of flow conditions (hysteresis delays nucleation to D in some cases). Following the **ONB** condition, heat transfer is by combined nucleation and convection modes in the region C-E (Partial Boiling). Finally, beyond E, Fully Developed Boiling (FDB) is established in the region E-G, and heat transfer is entirely by nucleate boiling mode. Nucleate boiling in which bubbles are formed by nucleation at the solid surface. In highly sub-cooled boiling these bubbles rapidly collapse, transferring their latent heat to the liquid phase and thus heating it dawn towards the saturation temperature. Therefore, it required to know the boiling safety factor (**K**) to avoid sub-cooled nucleate boiling at clad surface. As the maximum clad temperature at the hot spot shall be lower than boiling temperature, K should be higher than unity.

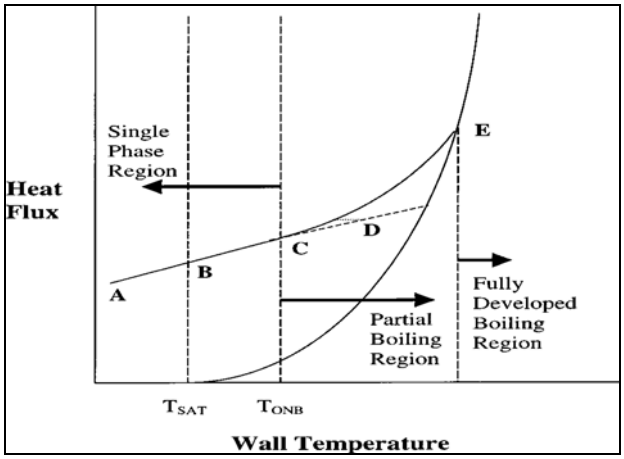

Fig (1): Heat flux dependence on wall superheat during sub-cooled flow boiling, (Kandlikar, 2003).

Young (1994) investigated experimentally in his study the critical heat flux (CHF) in transient boiling systems with vertical thin rectangular parallel plates

channel. One of the transient boiling systems is power transients. Power transient occurs when the heat generation rate or heat input varies with time. Generally, an increasing power transient is potentially disastrous and chaotic and is thus more important than a decreasing power transient. In the experiments related to forced convective boiling study, the primary parameters under investigation were transient modes, channel gap distances (3, 5 and 8 mm), inlet sub-cooling temperature (7.5 - 20.3) ^{o}C, mass flow rate (738 – 2162) kg/m2 sec and flow directions (Upward and downward). It is proved that as power is applied to the section as a function of time, the temperature and heat flux increase slowly at first and then very rapidly.

David and Issam (1996) predicted CHF correlations applicable to sub-cooled flow boiling in a uniformly heated vertical tube. They published in handbooks as well as the most recent correlations analyzed with the PU- BTPFL CHF database, which contains 29718 CHF data points. The parametric ranges of the CHF database are diameters from (0.3 to 45) mm, length-to-diameter ratios from (2 to 2484), mass velocities from (0.01x 10^3 to 138 x 10^3) kg/m^2.sec, inlet sub-under change of many factors and give good response of the system output. Cooling from (0 to 347) °C, inlet qualities from (2.63 to 0.00), outlet sub-cooling from (0 to 305) °C, out let qualities from (-2.13 to 1.00), and CHF from (0.05 x 10^6 to 276 x 10^6) W/m^2. A correlation published elsewhere is the most accurate in both low and high mass velocity regions. In general, CHF correlations developed from data covering a limited range of flow conditions cannot extended to other flow conditions without much uncertainty.

$$CHF = \frac{GD}{4L} C_{p,ave} (T_{out} - T_{in}) \quad (1)$$

Braz (2000) studied the thermal hydraulic behavior of electrically heated rod during a critical heat flux transient. He analyzed the front propagation velocity for the drying out and rewetting processes during the occurrence of CHF in electrically heated rod. The electrically heated element simulates nuclear fuel rods model's during the transient by applying an electrical power step from steady state condition. He made heated rod (16 cm diameter and 100 cm length) from a Ni-Cr wire. He found the linear power density is increased by 10% from its steady state to reach the CHF at 4 sec then the electric power is cut off. He showed the effect of the pressure, mass flow rate, inlet temperature on the behavior of electrically heating rod and that this variable has more influence on the drying front velocity than on the rewetting one.

Tomio Okawa et al. (2003) predicted the critical heat flux in annular flow regime accurately through new set correlations for the film flow analysis. All the correlations adopted on experimental data. The (4375) data of CHF in forced flow of water in vertical uniformly heated round tubes were used to test the basic performance of the model. He compared between the calculated and measured critical heat fluxes and he showed that the predicated results by the present model agree with the experimental data fairly if the flow pattern at the onset of CHF condition is considered annular flow.

Wu et al. (2010) conducted experiments which used the water as working fluid with pressure ranging from 1 to 4 MPa, mass flow velocity from 56 to 145 kg/m^2 s and wall heat flux from (9 to 58) KW/m^2 to study the onset of nucleate boiling (ONB) in heated vertical narrow annuli with annular gap sizes (0.95, 1.5 and 2) mm. They found that the ONB sometimes occurs only on outer annulus surface, sometimes occurs only on inner annulus surface and sometimes occurs on both annulus surfaces. The heat flux of the other side has great influence on the heat flux of the ONB and the latter will decrease with the increase of the heat flux of the other side. It is also found that the heat flux of the ONB increases with the increase of the pressure, the mass flux and wall superheat. However, the heat flux of the ONB will decrease as the gap size increases in narrow annuli. They predicted the heat flux of the ONB in narrow annuli through a new correlation, which has good agreement with the experimental data.

THEORETICAL ANALYSIS

Flowing water in a vertical annulus subjected to transient forced convection effect in radial direction is presented for modeling. A one-dimensional model can be used to describe the transient forced convection heat transfer in vertical annuals, with inner radius r_i and outer radius r_o which has a configuration shown in figure (2). Water flow direction is assumed to be in the downward direction according to the experimental setup.

The following assumptions are used in the modeling

- Incompressible fluid.
- One dimensional in (z-axis) flow. There is only one non zero velocity component, namely that in the direction of flow, v_z thus, $v_r = v_\theta = 0$.
- The axial velocity is independent of the angular location; that is, $\frac{\partial v_z}{\partial \theta} 0$.
- Simultaneously developing hydrodynamic.

- No internal heat generation and heat dissipation.
- Neglecting viscous dissipation.

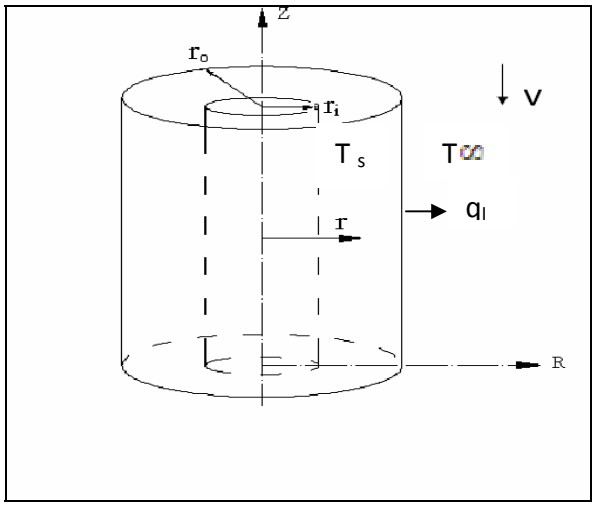

Fig (2): Axial annular geometry

FURTHER CALCULATIONS

To analyze the heat transfer process by forced convection from the heat source surface to the water flowing along it through annular section adjacent to the heat source surface simplified steps were used by conducting mass and heat balance at specified cross sectional area in the channel. The heat transfer coefficient is one of the affective parameters that should be estimated using the proper equations, Calculation procedure is conducted as follows:

- The total input power supplied to the wall can be calculated as;

$$q_t = V * I \quad (2)$$

- The heat loss (q_l) from the annular channel to the surrounding can be found from the following relation:

$$q_l = \frac{T_s - T_\infty}{\frac{1}{hA} + \frac{\ln(\frac{r_o}{r_i})}{2\pi k_g} + \frac{1}{h_{ins} A_o}} \quad (3)$$

The outer heat transfer coefficient of insulated cylinder (h_{ins}) is found using the following equation, **(Harlan and Bengtson, 2010)**. The correlation for Nu adopted for laminar flow at $(Ra \leq 10^9)$ is:

$$Nu = 0.68 + \frac{0.67 \cdot Ra^{.25}}{[1+(\frac{.492}{Pr})^{9/16}]^{4/9}} \quad (4)$$

$$Gr = g\beta L^3 \Delta T/\vartheta^2 \quad (5)$$

$$Pr = (\frac{\mu C_p}{k})_\infty \quad (6)$$

$$Ra = Gr * Pr \quad (7)$$

$$h_{ins} = (Nu * k_\infty)/(z) \quad (8)$$

- Heat transferred to the flowing water by convection is calculated by the following relation;

$$q_c = q_t - q_l \quad (9)$$

- Convective heat flux is calculated by using the following relation;

$$q'' = q_c/A_s \quad (10)$$

$$A_s = \pi D_i L \quad (11)$$

The Input parameters related to the total power of the heat source, hydraulic diameter, water volumetric flow rate, channel geometry and inlet water temperature are based on the experimental data that are used during the experimental part of the study. The target from theoretical study is to ensure certain model that predicts the measured parameters during experiments that uses power ranges higher the heater capacity. This insurance is validated by comparing the experimental and theoretical results to calculate the differences between them.

BULK WATER TEMPERATURE

To determine the bulk water temperature at the six points and compare them with the six thermocouple read out fixed along heater tube wall during study state condition, the following calculations are conducted;

$$T_{i+1,st} = T_{i,st} + \left(\frac{q'' \pi D_i z}{\dot{m} cp}\right) \quad (12)$$

The bulk water temperature during transient condition at any section of the annular gap at any time

could be derived from the following heat balance and as shown in figure (3):

Heat balance:

Inlet heat rate – outlet heat rate = accumulated heat

$$q_{i,tr}(t) - q_{l,tr}(t) + \dot{m}C_p T_{i,tr}(t) - \dot{m}C_p[2$$

$$T_{ave,tr}(t) - T_{i,tr}(t)] = MC_{p,ave}\frac{\partial T_{ave,tr}(t)}{\partial t} \quad (13)$$

$$T_{ave,tr}(t) = \frac{[T_i(t) + T_{i+1,tr}(t)]}{2} \rightarrow T_{i+1,tr}(t) = 2T_{ave,tr}(t) - T_i(t) \quad (14)$$

$$T_{ave}(t) = T_{ave,tr}(t) + T_{ave,st} \quad (15)$$

$$T_i(t) = T_{i,tr}(t) + T_{i,st} \quad (16)$$

$$T_{i+1}(t) = T_{i+1,tr}(t) + T_{i+1,st} \quad (17)$$

$$q_i(t) = q_{i,tr}(t) + q_{i,st} \quad (18)$$

$$q_l(t) = q_{l,tr}(t) + q_{l,st} \quad (19)$$

The equation [13] derived for specified element of bulk water within the annulus and solved by using Laplace method by using the transient part of the above equations [14, 15, 16, 17, 18 & 19] to investigate the transient part at node

$$T_{ave,tr}(s) = \frac{\Delta q}{s(\tau s + 1)(c1 + 2\dot{m}C_p)} + \frac{c1c2}{(\tau s + 1)(c1 + 2\dot{m}C_p)} + \frac{2\dot{m}C_p T_{i,tr}(s)}{(\tau s + 1)(c1 + 2\dot{m}C_p)} \quad (20)$$

Where:

$$\Delta q = \frac{q_t * \%\text{power increase} * c(z_{i+1} - z_i)}{L}$$

$$c1 = \frac{1}{[R_{the} + R_{the,con} + R_{the,ins}]} \qquad c2 = T_\infty$$

$$R_{the} = \frac{1}{hA}, \quad R_{the,con} = \frac{\ln\left(\frac{r_o}{r_i}\right)}{2\pi k_g}, \quad R_{the,ins} = \frac{1}{h_{ins}A_c}$$

$$\tau = \frac{MC_p}{c1 + 2\dot{m}C_p}, \quad M = \rho_{ave}a(z_{i+1} - z_i)$$

The eq. [20] derived to find the transient accumulated heat;

$$T_{ave,tr}(t) = \frac{\Delta q}{(c1 + 2\dot{m}C_p)}\left[1 - e^{-\frac{t}{\tau}}\right] + \frac{c1c2}{\tau(c1 + 2\dot{m}C_p)}e^{-\frac{t}{\tau}} + \frac{2\dot{m}C_p e^{-\frac{t}{\tau}}}{\tau(c1 + 2\dot{m}C_p)}T_{i,tr}(t) \quad (21)$$

$T_{ave,tr}(t)$ Substituent in eq. [14] to find $T_{i+1,tr}(t)$

$T_{i+1,tr}(t)$ Substituent in eq. [17] to find $T_{i+1}(t)$.

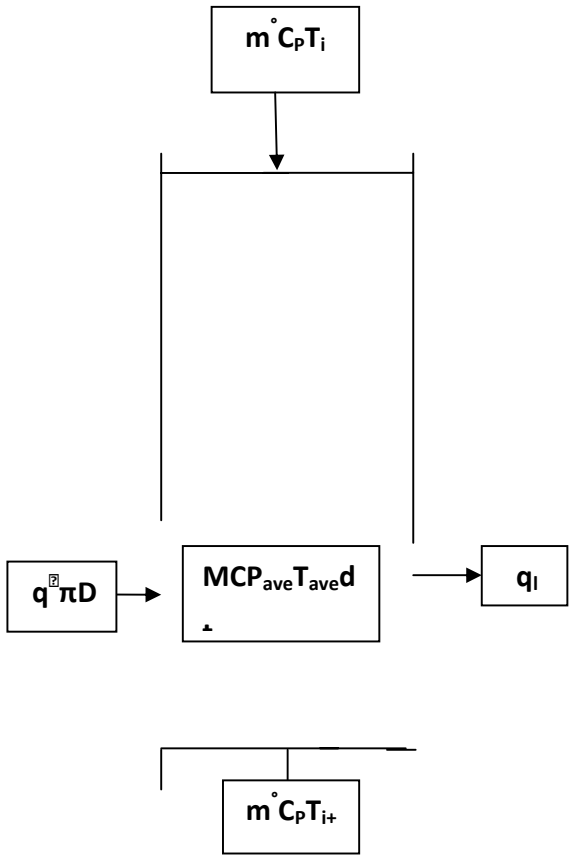

Fig (3): Heat balance mass transfer

LOCAL HEAT TRANSFER COEFFICIENT:

In order to investigate if the flow in the test section is fully developed or developing flow, it is necessary to estimate the thermal entrance length, The thermal entrance length (Z_{et}) given by the following expression; **(Ebadian and Dong 2006).**

$$\frac{Z_{et}}{D_h} = 0.034\,Re\,Pr \quad (22)$$

The following equation is used to calculate the heat transfer coefficient as shown below, **(EL-Wakil, 1962).**

$$h = \frac{0.021 C_{p,b} G (1+\frac{2.3 D_h}{L})}{(\frac{D_h G}{\mu_f})^{.2} Pr_f^{.66} (\frac{\mu_s}{\mu_b})^{.14}} \quad (23)$$

The thermal properties $(C_{p,b}, Pr_f, \mu_f, \mu_b \& \mu_s)$ in the eq. [27] is calculated from the heat transfer tables at film, bulk and clad surface temperatures $(T_f, T_{i-1}(t) \& T_s)$;

Where:

$$T_f = \frac{T_s + T_{i-1}(t)}{2} \quad (24)$$

$$T_s = T_{i-1}(t) + \frac{q''}{h} \quad (25)$$

To avoid sub-cooled nucleate boiling at clad surface, the maximum clad temperature at the hot spot shall be lower than boiling temperature. A safety factor (K) given by the following equation. **K** used to estimate this temperature; **(Ezzat and Taki, 1988).**

$$K = (T_B - T_{in})/(T_s - T_{in}) \quad (26)$$

Sub-cooled nucleate boiling of the coolant starts the heat source clad surface temperature reach to the boiling temperature at that position; T_B the following correlation is used for T_B estimation;

$$T_B = T_{sat} + 2.03 * q''^{0.35} * P^{-0.23} \quad (27)$$

$$P = P_i + \rho g z + (f \frac{z}{D_h}) . (\frac{v^2}{2g}) \quad (28)$$

EXPERIMENTAL WORK

The experimental work was conducted in the Heat Lab in the Mechanical Engineering department at Baghdad University. The design of the heat source simulates IRT-5000 research reactor by utilizing an electrical heater inside the heating element. The heating element is subjected to step power increase higher than its steady state value by around (5%- 20%) of its nominal power rate. The estimated heat flux based on 5 MW power of the research reactor was out of the capability of the heater used for simulation during the experimental part of the study. Therefore only 20% of this power is used during the experiments to ensure the integrity of the heat source. The water volumetric flow rate is fixed during the experiments at certain value that ensures the same temperature distribution along the heat source during steady state condition. While the inlet water temperature and other operational parameters are fixed as used in IRT 5000 reactor. The geometry of the heat source which is used during the experiments was cylindrical shape which is different from plate shape used in IRT-5000 reactor, due to fabrication difficulties. It consists of heat source consists of a nickel-chrome wire, wounded as (U) shape coil inside solid stainless steel cylinder and the stainless steel tube is fitted with thermal cement to isolate this coil from the stainless steel cylinder. The length of the heater is (70 cm), but the active heating length is (66cm), the diameter is (2 cm), the maximum total power is (2500 W), resistance of heat source (19.2Ω) and the maximum applied voltage (220-240) Volt. The flowing channel is made of Perspex glass to minimize the heat lost to the surrounding air due to its low thermal conductivity in addition to its transparency to enable visualization the flow patterns during water phase change. The cylindrical channel thickness is (1 cm), its length is (70 cm), with inner diameter equals (2.5 cm) and outer diameter equals (4.5 cm). To ensure the gap between two concentric cylinders equal to (0.25cm), proper flanges made from Teflon are fitted in the both ends of the cylindrical channel to resistant the high temperature caused by the effect of the heat source in the top and bottom of the annular channel. The temperature of the outside surface of the inner cylinder heat source is measured by using sixth asbestos sheath alumel-chromel (type T) thermocouples installed in six spaces (6.5, 19.5, 32.5, 45.5, 58.5 and 66) cm arranged along the heated wall. The digital thermometer type (12 channel temperature recorder with SD Card Data Logger) was used. The supplied water to the annular test section is heated up to 45°C in a rectangular cross section tank. The tank dimensions are (120×60×40) cm which is used to heat up the water in the circulation loop to the inlet temperature of the annular test section channel. The tank is constructed of (0.4 cm) thick AISI stainless steel. It is open from the top and consists of six orifices. The purpose of the orifices is to control the hydraulic behavior of the water which is used for cooling the heat source passing through the channel. See figure 4. The tank is equipped with a gate of (40×40) cm dimensions fixed at (10 cm) height from the bottom of the tank. The gate could be dismantled easily using proper bolts and gasket. The purpose of this gate is to facilitate the accessibility to the annular test section channel during experiments. The power of electrical heater 3000 W, (13Amp and

220 Volt) located at (10 cm) from the bottom of the tank to heat the water to its inlet temperature (45℃), see plate 1. The tank is connected to the cold water inlet which is supplied from cold water tank fixed at level higher than original tank level. The dimensions of the cold water tank are (40 cm) diameter and (100 cm) length, see plate 2. The water in the main tank is mixed with the cold water added to it before the circulation of the water in the annular test section channel to ensure the (45℃). The temperature of the water in the inlet of the annular test section channel is fixed at (45℃), while the inlet pressure is fixed at (1.05 bar) ensured by adjusting the control valve in the inlet of the annular test section channel. Heat exchange in the channel is ensured by forced convection between circulating water and the heat source of (2500 W). The water is circulated through the closed loop, where, the water is withdrawn from the suction pipe fixed at (10 cm) from the bottom of the tank at temperature (45℃). The water that exits from the pump is divided between the test section and the bypass pipe. The purpose of the bypass pipe is to control water flow rate and pressure in the channel through a control valve. The feed pipe consists of a flow meter (1-7 l/min) to read water flow rate in the test section channel. A pressure gage whose range is (0-100 kPa) is used to measure the inlet pressure of the water. The manometer used to read the pressure across different locations in the test section. Additional thermocouples are installed inside the channel to measure water temperature in the inlet and the outlet of the channel. To predicate the CHF phenomena during transient conditions it is planned to either decrease water velocity in the annular test section channel or increase the temperature of water at the inlet of the test section, as power increase is limited to the capability of the heat source to withstand the input current. Different water flow rates ranging (0.5 – 1) l/min are used during the experiments, while the inlet water temperature to the annular test section is ranged (55 – 75) ℃. Water flow pressure at distances (45.5, 58.5 and 65) cm from the heated wall inlet are measured by the water manometer during the power increase transient course at each water flow rate and water inlet temperature. When the pressure at any of these points starts to fluctuate sharply it predicts the transition of boiling configuration from nucleate boiling to film boiling at distance located upper from the pressure fluctuation point. The heat source power that initiates this fluctuation together with the related pressure measurements at the 3 above mentioned points, surface temperature and water temperature at these points are recorded versus the water inlet temperature and water flow rate.

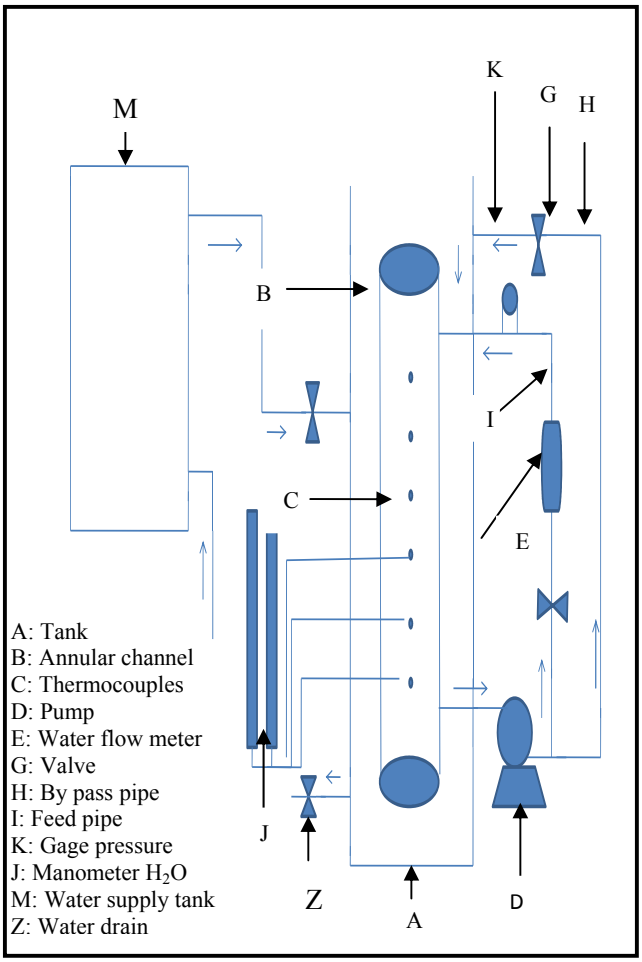

Fig (4): Diagram of annular test rig

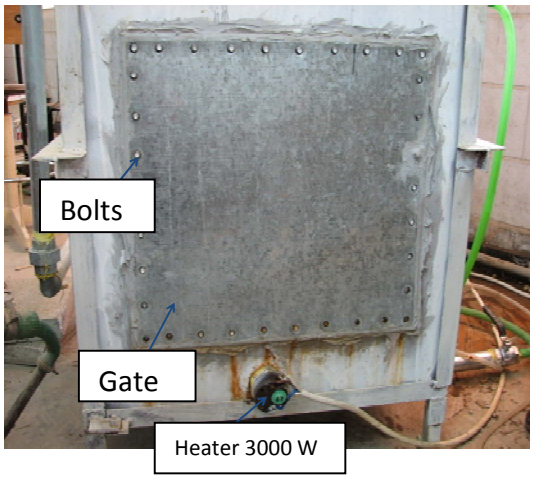

Plate (1): Test rig -back view

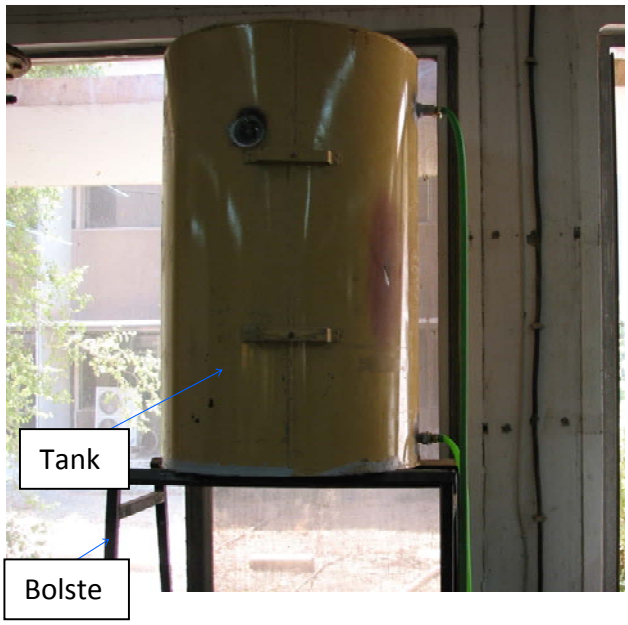

Plate (2): cold supply water tank

RESULT AND DISCUSSION

The adopted values of the total electrical power during the experiments are ranged (1920-2300) W which ensured heat flux values range (46.4-55.6) KW/m^2. The selection of heat flux range is limited to the above mentioned upper limit due to the limitation of the maximum available electrical power supplied to the heat source and the limitation of the material used to fabricate both the electrical source and its outer channel including the capability of the adhesive materials used to fix the thermocouples which starts to melt at temperatures exceed 120°C. Therefore the maximum value of heat flux didn't exceed 55.6 KW/m^2. The temperature variation along the heat source clad surface is plotted in figure 5. The figure shows the experimental and theoretical distribution of the surface temperature along electrical heat source at heat flux equal 1920 W during steady state condition. This figure reveals that the surface temperature increases starting from the annulus entrance and attains a maximum value at the end of the channel, point (65 cm). The rate of surface temperature increase is linearly proportional to the distance. Figure 6 shows the effect of 20% power increase transient respectively on the heat source clad surface temperature at the end of the electrical heat source, (65 cm). The figure shows that the maximum surface temperature is measured and calculated in the end of the heat source due to the effect of the increasing water bulk temperature affected by the accumulated heat added to the channel. The experimental and theoretical results related to the heat source clad surface temperature versus the elapsed time required to reach these temperatures to their steady state values at the end of the heat source, 65 cm are plotted. Figure 7 represents the curves plotted for power increase transient conditions (5%, 10%, 15% and 20%) of the nominal steady state power. It is clear that the clad surface temperature after reaching to their steady state values are proportional to power increase percentages, as these temperatures are directly proportional to the constant heat flux. Figure 8 shows the experimental and theoretical distribution of the bulk water temperature along heat source at power equal 1920 W during steady state condition. The bulk temperature is proportional directly with the distances (6.5 to 65) cm at constant heat flux (q''= 46376.8 W/m^2). The water bulk temperature reaches its maximum value at the end of the heat source, 65 cm due to the proportionality of the accumulated heat addition versus the channel distance. The figure shows that all bulk water temperatures are far from 100°C, water saturation temperature, while the degree of sub-cooling decreases along the heat source due to the continuous power addition. Figure 9 shows the experimental and theoretical bulk water temperature versus elapsed time required to reach the steady state condition at the end of the heat source, (65 cm) at 20% power increase transient. The figure shows that the maximum bulk water temperature measured and

calculated at the end of the heat source is proportional to the power increase rate due to the effect of the accumulated heat added to the channel. Figure 10 shows the experimental and theoretical values of the heat transfer coefficient versus the elapsed time required to reach the steady state condition at the end of the heat source, (65 cm) during 20% power increase transient. Comparison between heat transfer coefficient values after reaching to their steady state values demonstrates that these values are proportional to power increase percentages due to the effect of average bulk water velocity increase along the channel affected by water density decease to ensure continuity provision. The results reveal also that heat transfer coefficient increase the rate versus time is proportional also to the power increase percentages which justify the reason for the positive effect of power increase on the enhancement of the heat transfer process during nucleate boiling up to the point of departure from nucleate boiling, DNB. Figure 11 shows the boiling safety factor, K versus the elapsed time to reach steady state condition at the end of the heat source, (65 cm) after 20% power increase transients. It is clear that the decrease in K values versus elapsed time is due to the increase of the clad surface temperature versus power increase. The figure illustrates that power increase transient up to 15% of the nominal power during the recent experiments keeps **K** values above 1 till the end of the channel which excludes any possibility for nucleate boiling during these transients, while at 20% power increase transient K value goes below 1 which means ensuring of nucleate boiling at the end of the channel. To investigate the effect of higher power increase transients on the boiling safety factor and their related parameters, the heat source is assumed to be exposed to (30%, 40% and 50%) power increase percentages of its nominal power and the related parameters are studied theoretically only due to the limitation of the heat source to 20% power increase which bounded the experimental range. Figure 12 shows the comparison among curves related to theoretical results of the heat source clad surface temperature and bulk water temperature. These curves are plotted versus different power increase percentages (5% to 50%). It is clear that the elapsed time required for the bulk temperature to reach their steady state values are higher than those related to clad surface temperature and the slop of their curves are smoother which means that the response of any safety system to such power transients are more effective when their temperature sensors are linked to surface clad rather than bulk water. Figure 13 show the boiling safety factor at the end of the heat source surface (65 cm) at different percentage power increase (20%, 30%, 40% and 50%), respectively. It means that the elapsed times are proportional to the power increase percentages. This proportionality may leave linearity due to effect of the nucleate boiling phenomenon. There are several experimental methods to predict the critical heat fluxes. The first method depends on clad temperature observations during power increase transients. During applying this method, the heat flux is nominated as critical heat flux when its existence leads to sharp increase in clad temperature due to the poor heat transfer mechanism between the bulk fluid and clad surface affected by the progress of the nucleate boiling phase to film boiling phase. The second experimental method depends on the observation of the local water temperature along the heat source length. The position at which this pressure oscillates sharply will refer to the position of the DNB and the heat flux that leads to this oscillation will be nominated as critical heat flux. During the present experiments the second methodology is applied for prediction of critical heat flux. Figures 14 &15 show the experimental investigation of the effect of the water flow rate and the degree of water sub-cooled temperature respectively, on the critical heat flux **CHF** at which water starts to leave nucleate boiling at the clad surface hot spot temperature and pass to film boiling phase. Keeping each of the above two parameters constant during studying the effect of the other parameters on **CHF**, both curves show that critical heat flux is proportional directly with the water flow rate and with the sub-cooled water temperature. Figure 16 shows the pressure differences along the heat source water channel between their values during nominal power operation and those measured when the film boiling occures at departure from nucleate boiling, **DNB** postions during different water flow rates. These values obtained at water inlet temperature equals 60 °C. As discussed before as the water flow rate decreases the critical heat flux decreases at constant water inlet temperature and the position at which the film boiling initiates decreases. Accordingly, and as shown from the relevant figure, the slope of the pressure differences curve decreases also which means that the response time of any pressure sensor is proportional to water flow rates but however the sensitivity of this response is

inversely proportional to them. Figure 17&18 show the comparison between the experimental results obtained from the relevant experiments with those obtained using the correlation investigated by (David and Mudawar, 1996). Both figures investigate respectively the effect of the difference between inlet and outlet bulk water temperature and the water mass flux on the CHF. Keeping each of the above two parameters constant during studying the effect of the other parameter on CHF, both curves show that critical heat flux is proportional directly with the water mass flux and with the difference inlet and outlet bulk water temperature. The figures show some sensible differences with the relevant experimental results due to the differences in the applied operational pressure in the channels used during experiments.

CONCLUSIONS:

Heat transfer process improve versus power increase percentage transient due to the effect of nucleate boiling which depends on the nominal power rate, power increase percentage , coolant mass flow rate and channel geometry. The heat source is affected by the action of the hydraulic behavior of the water coolant (bulk water temperature, drop of the water pressure) where, the bulk water temperature and drop in the pressure due to the friction reaches their maximum values versus distance.

1. The nucleate boiling phenomena occurred only in case 20% power increase transient as the boiling safety factor was reached to equal (1) at the end of the heat source, .65 m at (10 sec), which means that power protection sensor should use the power increase percentage as threshold for its activation.
2. As the power source is constant heat flux, clad surface temperature reaches its maximum value at the end of the heat source, (0.65 m) in power increase transient which means that any power transient prediction should be fixed at the end of the channel.
3. The surface temperature response is faster than that related to bulk water temperature affected by power increase transient which means that any safety system response to such power transients are more effective when their temperature sensors are linked to surface clad rather than bulk water.
4. The critical heat flux, CHF is proportional to the mass flow rate of the coolant, while it is inversely proportional to channel inlet water temperature. There are more factors which affect the value of CHF as, channel length, diameter and water pressure inside the channel.

NOMENCLATURE

A_o	Surface area of channel
A_s	Surface area of heat source
c	Circumference of heat source **($c=\pi D_i$)**
c1&c2	Constants
C_p	Specific heat of constant pressure
D_i	Inner diameter of heat source
D_o	Outer diameter of channel
D_h	Hydraulic diameter= (D_o-D_i)
f	Friction factor (f= 64/ Re)
g	Gravity acceleration
G	Mass velocity of water
Gr	Grashof number
h	Heat transfer coefficient
I	Current
k_g	Thermal conductivity of the insulated channel
K	Boiling safety factor
L	Length of heat source
m°	Mass flow rate of water
M	Mass of water
P	Pressure
P_i	Inlet pressure at the top of the channel
pr	Prandtl number
q_c	Convective heat to the water
q_l	Heat lost to the surrounding air
q_t	Total heat power
q''	Heat flux
Ra	Rayligh number
r_i	Inner radius of the insulated channel
r_o	Outer radius of the insulated channel
Re	Reynolds number
Q	Flow rate of water
t	Time
T	Temperature
τ	Time Constant
v	Axial velocity
V	Voltage
z	Axial distance along heat source
z_{et}	Thermal entrance length

GREEK LETTERS

β	Coefficient of volume expansion
ϑ	Kinematic viscosity
ρ	Density

SUBSCRIPT

∞	Surrounding air around channel
ave	Average
b	Bulk
in	Inlet water
ins	Insulator
out	outlet water
sat.	Saturated
st	Steady state condition
tr	Transient
the.con	Theoretical conduction heat transfer

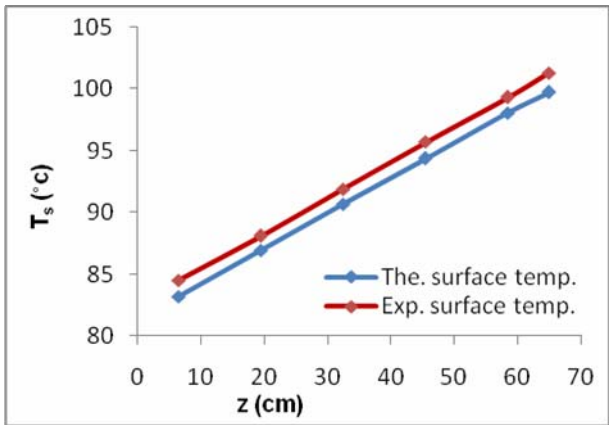

Fig 5: Experimental and theoretical clad surface temperature versus distance during steady state condition.

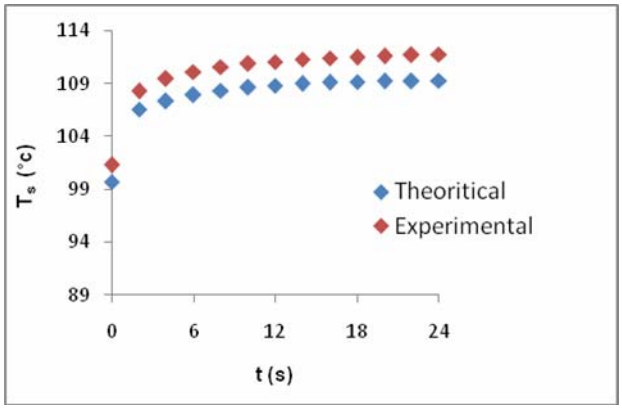

Fig 6: Theoretical and experimental clad surface temperature versus time at the end of the heat source, (65 cm) during 20% power increase transient.

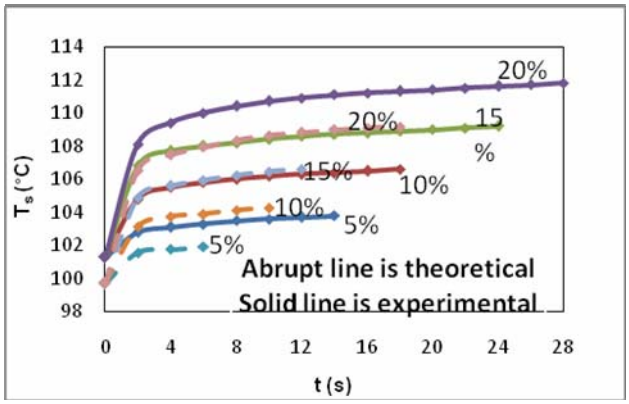

Fig 7: Experimental and theoretical surface temperature versus time at the end of the heat source, (65 cm) during (5%, 10%, 15 and 20%) power increase transient.

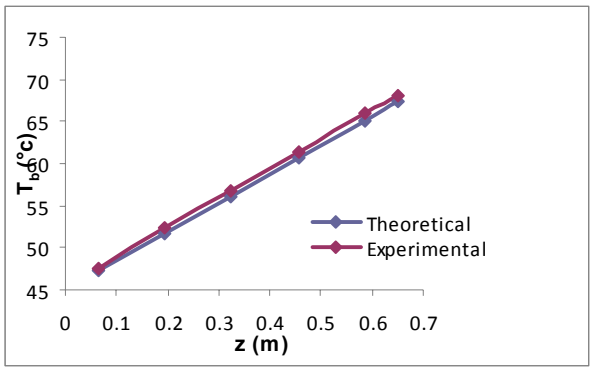

Fig 8: Experimental and theoretical bulk water temperature versus distance during steady state condition.

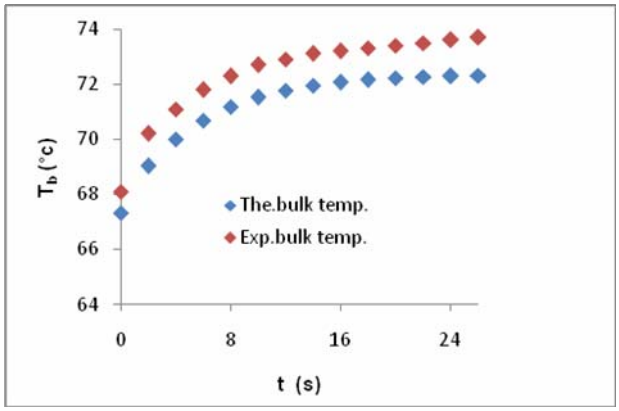

Fig 9.Theoretical and experimental bulk water temperature versus time at the end of the heat source (65cm) during 20% power increase transient

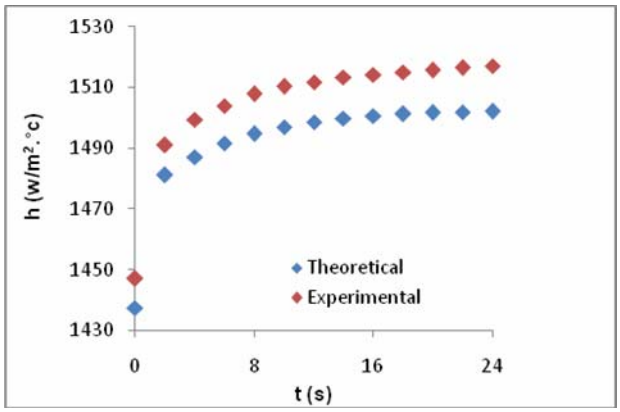

Fig 10: Theoretical and experimental heat transfer coefficient versus time at the end of the heat source, (65 cm) during 20% power increase transient.

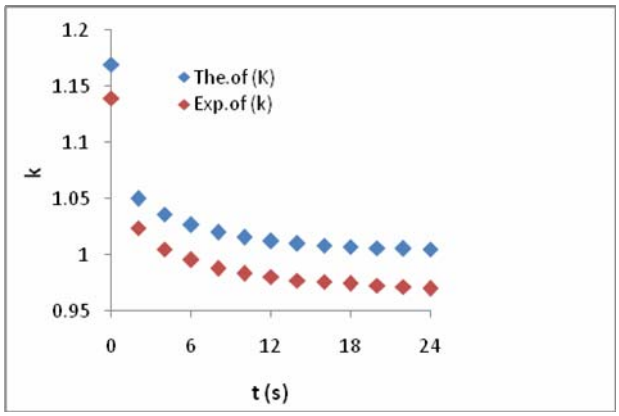

Fig 11: Theoretical and experimental boiling safety factor versus time at the end of the heat source, (65 cm) during 20% power increase transient.

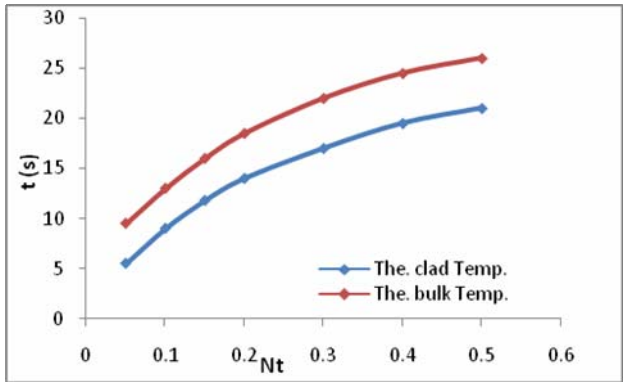

Fig 12: Theoretically measured elapsed time required to reach steady state surface clad and water bulk temperature at the end of the heat source, (65 cm) versus (5%, to 50%) percentage power increase transient.

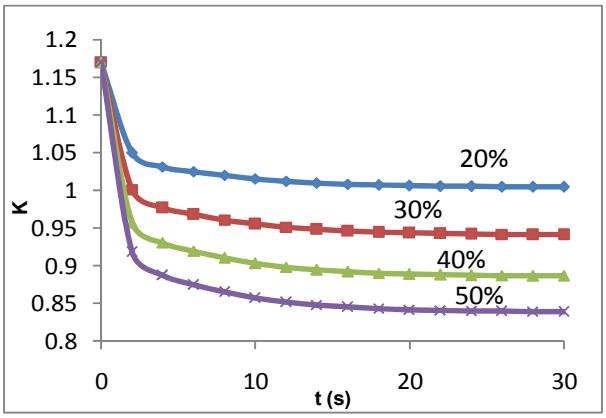

Fig 13: Theoretical boiling safety factor, K versus time at the end of the heat source, (65 cm) during 20%, 30%, 40% and 50% power increase transient.

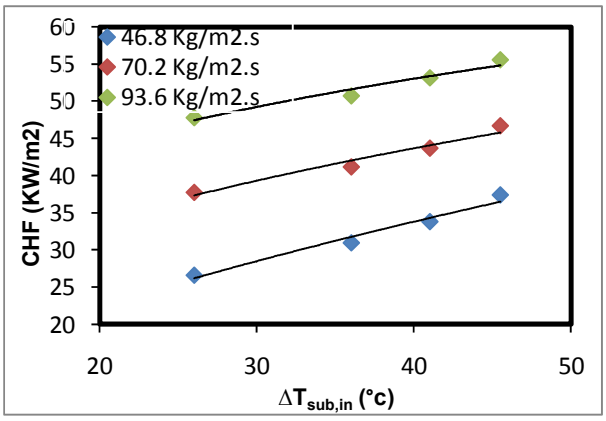

Fig 14: Experimental CHF versus inlet sub-cooled water temperature at different inlet water flow rate

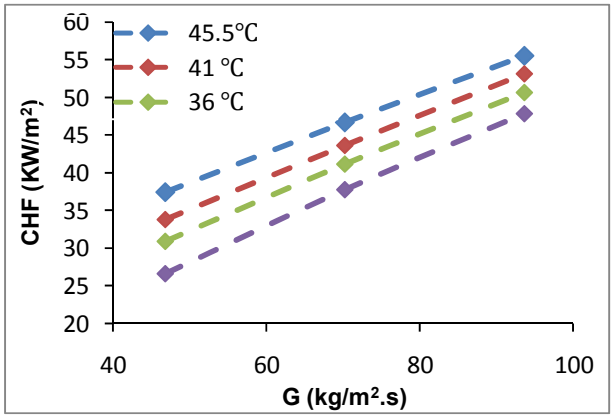

Fig 15: Experimental CHF versus mass flux of water at different sub-cooled water temperature.

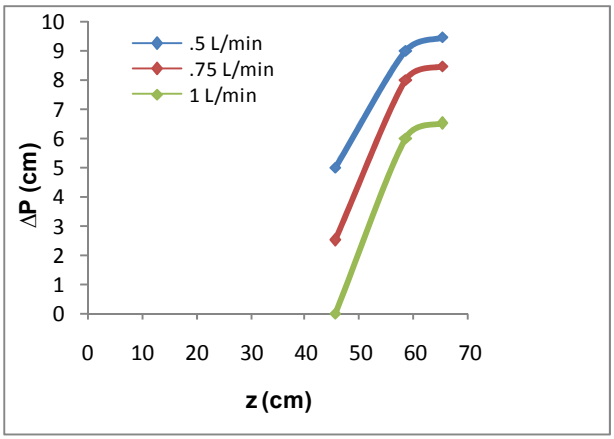

Fig 16: Pressure difference versus distance (45.5, 58.5 and 65) cm at inlet water temperature (60°C) in the steady state condition

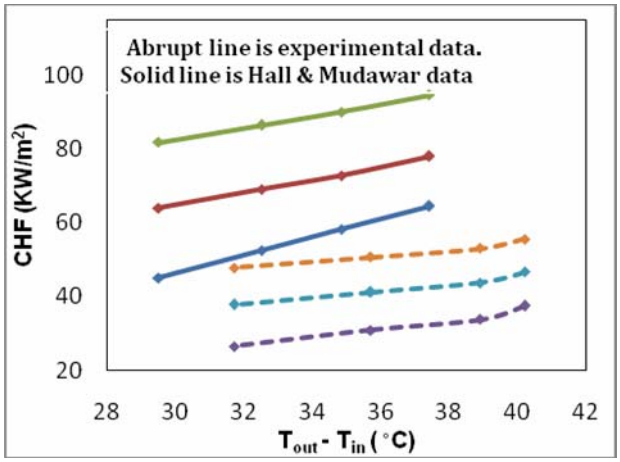

Fig 17: Comparison of experimental data with existing correlation (critical heat flux versus difference between inlet and outlet bulk water temperature for different mass flux).

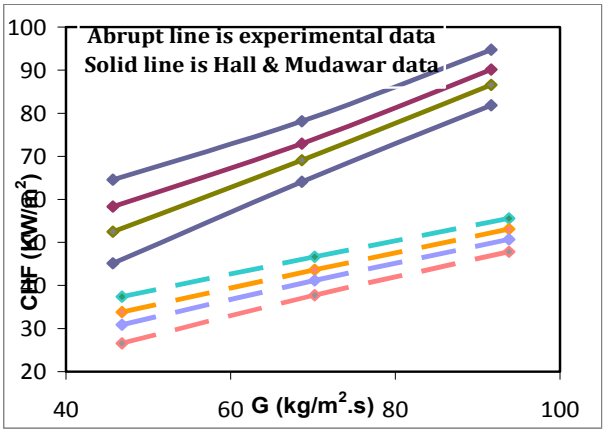

Fig 18: Comparison of experimental data with existing correlation (critical heat flux versus mass flux for different difference between inlet and outlet bulk water temperature ($T_{out} - T_{in}$)).

REFERENCES

A.W.Ezzat and H.M.Taki. (1988) Final safety report for 14th Tammuz 5000 KW reactor, INC, Iraq nuclear commission under the supervision of IAEA, paragraph 5.4.

David D.Hall and Issam Mudawar. (1996) "Evaluation of subcooled critical heat flux correlations using the PU-BTPFL CHF database for vertical up flow of water in a uniformly heated round tube", Boiling and Two-Phase Flow Laboratory, School of Mechanical Engineering, Indiana 47907-1288.

Dr.Harlan H.Bengtson, P.E. (2010) "Convection heat transfer coefficient estimation" www.SunCam.com, PP. 2-40.

J. Braz. (2000) " Thermal hydraulic behavior of electrically heated rod during a critical heat flux transient"Journal of Brazilian Society of Mechanical Sciences and Engineering, Vol. 22 No.4, ISS 0100-7386.

M.A.Ebadian and Z.F.Dong, (2006) "Forced convection, internal flow in ducts "Chapter 5, Florida International University.

M.M.El.Wakil. (1962) "Nuclear Power Engineering " McGraw-Hill Book Company, New York.

Tomio Okawa, Akio Kotani, Isao Kataoka and Masanori Naito, (2003), "Prediction of critical heat flux in annular flow using a film flow model" Journal of Nuclear Science and Technology, Vol.40, No.6, PP. 388-396.

Yong Tae Kang, B.S., M.S. (1994) "Experimental investigation of critical heat flux transient boiling systems with vertical thin rectangular parallel plate channels" Ph.Sc.Thesis, School of the Ohio State University.

Y.W.Wu, G.H.Su, B.X.Hu and S.Z.Qiu, (2010) "Study on onset of nucleate boiling in bilaterally heated narrow annuli" International journal of Thermal Sciences, Vol.49, PP. 741-748.